HHS Public Access

Author manuscript

Nat Immunol. Author manuscript; available in PMC 2015 November 28.

Published in final edited form as:

Nat Immunol. 2005 August ; 6(8): 800–809. doi:10.1038/ni1228.

Loss of adenomatous polyposis coli gene function disrupts thymic development

Fotini Gounari[1], **Rui Chang**[1], **Janet Cowan**[2], **Zhuyan Guo**[1], **Marei Dose**[1], **Elias Gounaris**[3,4], and **Khashayarsha Khazaie**[3,4]

[1]Molecular Oncology Research Institute, Tufts–New England Medical Center, Boston, Massachusetts 02111, USA

[2]Department of Pediatrics, Tufts–New England Medical Center, Boston, Massachusetts 02111, USA

[3]Dana Farber Cancer Institute, Harvard Medical School, Boston, Massachusetts 02115, USA

[4]Center for Molecular Imaging Research, Massachusetts General Hospital and Harvard Medical School, Charlestown, Massachusetts 02129, USA

Abstract

Loss of the adenomatous polyposis coli (APC) protein is a common initiating event in colon cancer. Here we show that thymocyte-specific loss of APC deregulated β-catenin signaling and suppressed Notch-dependent transcription. These events promoted the proliferation of cells of the double-negative 3 and 4 stages and reduced rearrangements between the variable, diversity and joining regions of the gene encoding T cell receptor (TCR) β, encouraging developmental progression of aberrant thymocytes lacking pre-TCR and αβ TCR. Simultaneously, the loss of APC prolonged the mitotic metaphase-to-anaphase checkpoint and impaired chromosome segregation, blocking development beyond the double-negative 4 stage. The result was extensive thymic atrophy and increased frequencies of thymocytes with chromosomal abnormalities. Thus, loss of APC in immature thymocytes has consequences distinct from those of deregulation of β-catenin signaling and is essential for T cell differentiation.

Adenomatous polyposis coli (APC) is a tumor suppressor whose loss is intimately linked with colon cancer. APC is an essential component of the Wnt signaling pathway and is required for the formation of a cytoplasmic complex containing β-catenin, the kinase GSK-3β and axin. In this complex, β-catenin is phosphorylated by GSK-3β and is ‘tagged’ for degradation[1]. When Wnt signaling is activated by the binding of Wnt soluble proteins to frizzled receptors, this complex is disrupted and nonphosphorylated β-catenin is stabilized. The non-phospholylated β-catenin binds to the Tcf-Lef family of transcription factors and activates Wnt-dependent gene transcription by providing a transcription activation domain to the complex[1].

Correspondence should be addressed to F.G. (fgounari@tufts-nemc.org) or K.K. (khashayarsha_khazaie@dfci.harvard.edu).

COMPETING INTERESTS STATEMENT

The authors declare that they have no competing financial interests.

Supplementary information is available on the Nature Immunology website.

Most human colorectal tumors contain mutations in *APC*, although in rare instances those with an intact *APC* contain activating mutations of the gene encoding β-catenin that alter the functionally important phosphorylation sites[2–4]. The *APC* mutations result in truncated proteins that lack all axin-binding motifs and a variable number of the 20–amino acid repeats that are associated with down-regulation of intracellular β-catenin[5–7]. Those findings led to the idea that the main tumor-suppressing function of APC resides in its capacity to properly regulate intracellular β-catenin[2,3,8]. However, *APC* encodes a multifunctional protein that participates in several cellular processes, including cell adhesion and migration, signal transduction, microtubule assembly and chromosome segregation. In dividing cells, APC is localized at the kinetochore and interacts with the microtubule end-binding protein EB1 as well as the cell cycle checkpoint proteins Bub1 and Bub3 (refs. 9–11). It has been proposed that loss of APC may lead to chromosomal instability, which is a hallmark of colorectal cancer. The developmental consequences of loss of APC are not yet clearly understood.

There is indisputable evidence that the canonical Wnt–β-catenin signaling cascade is important in thymocyte development. T cells develop from bone marrow progenitors that migrate to the thymus[12–17] and commit to the T cell lineage after stimulation of Notch signaling by Delta-like ligands[18,19]. At the $CD44^{-}CD25^{+}$ double-negative 3 (DN3) stage of development, productive rearrangement of the T cell receptor β (*Tcrb*) locus leads to the assembly of the pre–T cell receptor (pre-TCR), which signals survival, proliferation and differentiation, effectively ‘instructing’ pre–T cells to develop into the αβ T cell lineage[20]. *Tcrb* rearrangements by variable (diversity) joining (V(D)J) recombination in this stage depend on Notch1 signaling, as thymocyte-specific ablation of Notch1 leads to their supression[21]. Thymocytes express two members of the Tcf-Lef family: Tcf-1 and Lef-1. Ablation of Tcf-1 activity affects all proliferating stages of thymocyte development, including the $CD44^{+}CD25^{+}$ DN2 stage and the pre-TCR-dependent $CD44^{-}CD25^{-}$ DN4 stage[22]. The $Tcf1^{-/-}$ developmental block at the DN4 stage is β-catenin dependent, as it can be ‘relieved’ only by transgenic reconstitution with versions of Tcf that contain an intact β-catenin binding domain[23]. Concomitant ablation of Lef and Tcf-1 results in complete blockade of embryonic thymocytes at the immature single-positive stage[24]. Consistent with those findings, conditional ablation of β-catenin inhibits T cell development at the pre-TCR checkpoint[25]. However, conditional stabilization of β-catenin in DN3 thymocytes allows developmental progression in the absence of pre-TCR and αβ TCR[26].

We have examined here the developmental consequences of thymocyte-specific loss of APC function *in vivo*. Using two conditional mouse models, one permitting thymocyte-specific loss of APC function and the other allowing direct stabilization of β-catenin, we were able to demonstrate unique properties of APC that are vital to T cell maturation. Our observations show the devastating effect of APC deficiency on a developmental process that involves extensive cellular proliferation.

RESULTS

Thymocyte differentiation after loss of APC function

To characterize the function of APC on thymocyte development, we generated a mouse strain that allowed Cre-dependent conditional truncation of *Apc*. We flanked exons 11 and 12 of *Apc* with *lox*P sites (*Apc*^{lox468}; Fig. 1a). We achieved functional ablation of APC by Cre-mediated deletion of these exons, leading to out-of-frame splicing of exon 10 to exon 13 and the generation of a prematurely terminated 468–amino acid protein (APC$^{\Delta 468}$). This truncated product was shorter than most reported APC truncations[27–29]. Constitutive APC$^{\Delta 468}$ truncation was lethal when homozygous, and the heterozygous mice developed intestinal polyps starting at 2 months of age (unpublished observations). Deregulation of β-catenin signaling has been considered the chief consequence of the loss of APC in colon cancer. We compared thymic development after APC truncation with thymic development after expression of a stable β-catenin. We achieved stabilization of β-catenin by Cre-mediated excision of its third exon (*Ctnnb1*$^{lox(ex3)}$). Exon 3 of β-catenin encodes a protein of 76 amino acids and includes critical phosphorylation sites involved in the degradation of this protein. Its deletion allows the joining in-frame of exons 2 and 4 and expression of a functional dominant-acting stable β-catenin protein[26,30].

We achieved thymocyte-specific loss of APC function or stabilization of β-catenin by crossing those conditional gene-targeted mouse strains with a transgenic strain that expresses Cre under the control of the proximal *Lck* promoter (LckCre)[31]. To monitor the course of Cre-mediated deletion in compound mutant mice homozygous for the *Apc*^{lox468} allele and LckCre(LckCre-*Apc*$^{lox/lox468}$), we amplified DNA from sorted DN3 and DN4 thymocytes by PCR using primers detecting wild-type alleles, *lox*P-flanked alleles or deletion of *Apc* alleles (Fig. 1a). At the DN3 stage, LckCre-*Apc*$^{lox/lox468}$ thymocytes demonstrated a PCR product corresponding to the *lox*P-flanked allele, indicating that deletion was not complete. However, DN4 thymocytes yielded exclusively the PCR product corresponding to deletion of the allele, indicating that Cre-mediated deletion at this stage had reached completion (Fig. 1b).

APC is essential in the formation of the protein complex that is responsible for the phosphorylation-destruction of β-catenin[1], and in its absence, stable, nonphosphorylated β-catenin accumulates in cells. We therefore confirmed functional loss of APC by correlating the Cre-mediated truncation of *Apc* with increases in β-catenin. We compared the amount of β-catenin in APC-deficient thymocytes with that achieved through Cre-mediated excision of exon 3 of the gene encoding β-catenin. We analyzed lysates from LckCre and LckCre-*Apc*$^{lox/lox468}$ mice and heterozygous LckCre-*Ctnnb1*$^{+/lox(ex3)}$ mice by immunoblot using antibody to β-catenin (anti-β-catenin). LckCre-*Apc*$^{lox/lox468}$ and LckCre-*Ctnnb1*$^{+/lox(ex3)}$ thymocytes showed substantial accumulation of wild-type β-catenin and β-catenin lacking the section encoded by exon 3, respectively, greater than those in the LckCre single-transgenic thymocytes (Fig. 1c). We assessed the course of β-catenin accumulation during thymocyte maturation by intracellular β-catenin staining and flow cytometry (Fig. 1d). Starting at the DN3 stage of thymic development, steady-state β-catenin gradually increased in LckCre-*Apc*$^{lox/lox468}$ and LckCre-*Ctnnb1*$^{+/lox(ex3)}$ thymocytes and remained high in all

subsequent stages in contrast to that of LckCre mice or the heterozygous LckCre-*Apc*$^{+/lox468}$ control mice, in which it remained low throughout development. Accumulation of β-catenin in LckCre-*Apc*$^{lox/lox468}$ thymocytes closely resembled that of LckCre-*Ctnnb1*$^{+/lox(ex3)}$ thymocytes (Fig. 1c).

To elucidate the consequences of loss of APC function on thymic development and to compare those with the outcome of direct stabilization of β-catenin, we analyzed thymi from LckCre control and LckCre-*Apc*$^{lox/lox468}$ littermates as well as age-matched LckCre-*Ctnnb1*$^{+/lox(ex3)}$ mice for thymic cellularity, subset distribution, thymocyte survival and cell cycling. LckCre-*Apc*$^{lox/lox468}$ thymi were noticeably smaller, containing one eight to one tenth the thymocytes in LckCre control thymi and half as many thymocytes as those of age-matched LckCre-*Ctnnb1*$^{+/lox(ex3)}$ mice (Fig. 2a). We established the precise distribution of thymocyte subsets in these mice using flow cytometry (Fig. 2b). Over 50% of the LckCre-*Apc*$^{lox/lox468}$ thymocytes had a CD4^{-}CD8^{-} DN surface phenotype, compared with 3.3% for LckCre-*Ctnnb1*$^{+/lox(ex3)}$ and 2.4% for LckCre, indicating a considerable block at the DN stages of thymocyte development due to loss of APC function. The DN block was not related to stabilization of β-catenin, as DN cells failed to accumulate in LckCre-*Ctnnb1*$^{+/lox(ex3)}$ mice and required loss of both *Apc* alleles, as demonstrated by the unperturbed thymic development of heterozygous LckCre-*Apc*$^{+/lox468}$ mice (Fig. 2b). Quantification of each thymocyte subset indicated that the reduction in cellularity was not evenly distributed. Although absolute numbers of DN3 stage thymocytes were similar in LckCre-*Apc*$^{lox/lox468}$, LckCre-*Ctnnb1*$^{+/lox(ex3)}$ and LckCre mice, LckCre-*Apc*$^{lox/lox468}$ mice had two- to threefold more DN4 cells ($4.5 \times 10^6 \pm 0.8 \times 10^6$ cells; $P < 0.03$), indicating a substantial developmental block at this stage. This idea was further supported by the reduction in thymocyte numbers of all subsequent maturation stages.

Reduced thymic cellularity in LckCre-*Apc*$^{lox/lox468}$ mice may reflect reduced survival, as already seen in LckCre-*Ctnnb1*$^{+/lox(ex3)}$ mice[26]. We assessed the frequency of apoptosis after loss of APC function or stabilization of β-catenin by measuring the fraction of annexin V–positive cells in electronically gated thymocyte subsets. DN3, DN4 and CD4^{+}CD8^{+} (double-positive (DP)) thymocytes from both LckCre-*Apc*$^{lox/lox468}$ and LckCre-*Ctnnb1*$^{+/lox(ex3)}$ mice demonstrated consistently higher frequencies of apoptosis than those of LckCre control mice ($P < 0.07$; Fig. 3a). In addition, cumulative data indicated that LckCre-*Apc*$^{lox/lox468}$ DN4 thymocytes had only marginally higher frequencies of apoptosis than did LckCre-*Ctnnb1*$^{+/lox(ex3)}$ thymocytes ($P < 0.28$). To address the increased apoptosis mechanistically, we examined the expression pattern of the antiapoptotic protein Bcl-2 during the development of LckCre-*Apc*$^{lox/lox468}$, LckCre-*Ctnnb1*$^{+/lox(ex3)}$ and LckCre-*Apc*$^{+/lox468}$ thymocytes as well as LckCre control thymocytes by intracellular staining with anti-Bcl-2 and flow cytometry (Fig. 3b, thick lines). Two ‘waves’ of Bcl-2 expression have been reported during thymocyte development: one in DN pre–T cells and one in mature single-positive (SP) T cells[32]. DP thymocytes apparently have low expression of Bcl-2. In LckCre-*Apc*$^{lox/lox468}$ and LckCre-*Ctnnb1*$^{+/lox(ex3)}$ thymocytes, Bcl-2 expression was downregulated earlier than in LckCre control thymocytes, starting at the DN3 stage. LckCre-*Apc*$^{lox/lox468}$, LckCre-*Ctnnb1*$^{+/lox(ex3)}$ and LckCre thymocytes had comparably low Bcl-2 at the DP stage. This expression remained low in TCRβ^{-} CD4^{+} and CD8^{+} SP cells

from both LckCre-*Apc*$^{lox/lox468}$ and LckCre-*Ctnnb1*$^{+/lox(ex3)}$ mice. This deregulation of Bcl-2 explains in part the increased apoptosis of thymocytes resulting from loss of APC function or stabilization of β-catenin.

We assessed the effect of the APC truncation on thymocyte cycling using intracellular staining with the ratiometric DNA dye 7-amino-actinomycin D (7AAD) and flow cytometry[23]. We electronically gated thymocyte subsets and 'plotted' 7AAD staining to estimate the fraction of cycling cells (Fig. 3c). Both LckCre-*Apc*$^{lox/lox468}$ and LckCre-*Ctnnb1*$^{+/lox(ex3)}$ thymocytes showed an increased fraction of cycling cells at the DN3 stage that averaged 16.1% ($P < 0.0001$) and 16.9% ($P < 0.019$), respectively, compared with 9.2% for LckCre control cells (Fig. 3c). At the DN4 stage, cell cycling was reduced for both LckCre-*Apc*$^{lox/lox468}$ and LckCre-*Ctnnb1*$^{+/lox(ex3)}$ thymocytes (21.87%, $P < 0.0002$, and 23.4%, $P < 0.004$, respectively) compared with that of LckCre thymocytes (37%). To assess the possibility that decreased cell cycling at the DN4 stage may have been related to the lack of pre-TCR signaling, we compared intracellular TCRβ expression in immature thymocytes of LckCre-*Apc*$^{lox/lox468}$ and LckCre-*Ctnnb1*$^{+/lox(ex3)}$ mice. Only a few LckCre-*Apc*$^{lox/lox468}$ or LckCre-*Ctnnb1*$^{+/lox(ex3)}$ thymocytes had detectable intracellular TCRβ expression throughout thymocyte development from the $CD44^{-}CD25^{-}$ DN4 stage to the $CD4^{+}CD8^{+}$ DP stage as well as the $CD4^{+}$ and $CD8^{+}$ SP stages (Fig. 3d). This result is in agreement with the idea that β-catenin stabilization induced by loss of APC function promoted thymocyte development in the absence of pre-TCR and αβ TCR. Thus, APC is essential in thymic development. Loss of APC function in immature thymocytes resulted in a precise blockade at the DN4 stage of development, decreased survival of immature thymocytes due to downregulation of Bcl-2, and reduced cell cycling, probably due to the lack of intracellular TCRβ and pre-TCR signaling.

Suppression of *Tcrb* VDJ rearrangements by APC and/or β-catenin

Intracellular TCRβ chains were reduced in both LckCre-*Ctnnb1*$^{+/lox(ex3)}$ and LckCre-*Apc*$^{lox/lox468}$ thymocytes. However, it was not clear whether this resulted from impairment in *Tcrb* rearrangements or from suppression of *Tcrb* transcription. To distinguish those possibilities, we compared *Tcrb* rearrangements in sorted DN3 and DN4 thymocytes from LckCre, LckCre-*Apc*$^{+/lox468}$, LckCre-*Ctnnb1*$^{+/lox(ex3)}$ and LckCre-*Apc*$^{lox/lox468}$ mice (Fig. 4a). For this, we applied a combination of limited and quantitative PCR analyses. We used limited PCR analyses to visualize the overall amounts of *Tcrb* DJ and VDJ rearrangements in these cells and we used real-time PCR to quantify any differences[33]. Rearrangements involving the $V_{\beta}5.1$ segment were reduced to 4.4% (DN3) and 4.2% (DN4) in LckCre-*Apc*$^{lox/lox468}$ thymocytes and to 11.8% (DN3) and 5.6% (DN4) in LckCre-*Ctnnb1*$^{+/lox(ex3)}$ thymocytes compared with rearrangements in the equivalent subsets of LckCre mice, which we considered to be 100%. There were comparable reductions in rearrangements involving the $V_{\beta}8.2$ segment at the DN3 (16.1%) and DN4 (11.7%) stages in LckCre-*Apc*$^{lox/lox468}$ thymocytes and DN3 (20.4%) and DN4 (11.4%) stages in LckCre-*Ctnnb1*$^{+/lox(ex3)}$ thymocytes, compared with those of LckCre mice (Fig. 4b). Thus, the lack of TCRβ chains in most LckCre-*Apc*$^{lox/lox468}$ and LckCre-*Ctnnb1*$^{lox/lox(ex3)}$ developing thymocytes was the result of specific suppression of *Tcrb* V-to-DJ rearrangements in these cells, whereas DJ rearrangements were not affected (Fig. 4b).

β-catenin–Notch crosstalk affects *Tcrb* rearrangements

Conditional ablation of Notch1 impairs *Tcrb* V-to-DJ gene rearrangements, resulting in the development of DN3 and DN4 cells that have reduced intracellular TCRβ and mature in the absence of pre-TCR[21]. Interaction between the Wnt–β-catenin and Notch pathways has been proposed to have important consequences for the regulation of differentiation and self-renewal in other developmental systems[34–37]. To address the possibility that Notch activity may be regulated by the loss of APC and the resulting stabilization of β-catenin, we examined Notch-dependent transcription in sorted DN3 and DN4 thymocytes derived from LckCre-*Ctnnb1*$^{+/lox(ex3)}$ and LckCre-*Apc*$^{lox/lox468}$ mice. Semiquantitive RT-PCR for *Notch1* and *Notch3* as well as the Notch target genes *Hes1* and *Dlx1* indicated that both APC truncation and β-catenin stabilization resulted in a reduction in Notch-dependent transcription compared with that of LckCre control cells (Fig. 5). Downregulation of Notch-dependent transcription was evident in DN4 thymocytes, whereas similar suppression in DN3 cells was not detectable. This result may be related to incomplete Cre-mediated deletion in LckCre-*Ctnnb1*$^{+/lox(ex3)}$ and LckCre-*Apc*$^{lox/lox468}$ thymocytes and only partial accumulation of β-catenin at this developmental stage (Fig. 1b,d)

To directly determine whether crosstalk between the β-catenin and Notch pathways affected *Tcrb* VDJ rearrangements, we expressed activated Notch (NotchIC) in immature thymocytes from LckCre-*Apc*$^{lox/lox468}$ and LckCre-*Ctnnb1*$^{+/lox(ex3)}$ mice as well as from LckCre control mice and measured intracellular TCRβ expression after differentiation after culture of these cells together with OP9-DL1 stromal cells[19]. We magnetically selected CD25^{+} DN2 and DN3 cells and infected the cells with retroviruses expressing either NotchIC in the context of a bicistonic transcript including enhanced green fluorescent protein (EGFP) or EGFP alone[38]. We independently sorted infected EGFP^{+} as well as uninfected DN2 and DN3 cells (Fig. 6) and cultured the cells on OP9-DL1 stromal cells for 8–9 d. We collected cells from those cultures and stained them with anti-CD45 to identify the lymphoid cells and with anti-CD4 and anti-CD8 to define the cells that had matured during culture. We followed the surface staining with intracellular staining using anti-TCRβ and flow cytometry. We analyzed electronically gated CD45^{+}CD4^{+}CD8^{+} cells for intracellular TCRβ expression. Infection of immature thymocytes with NotchIC-expressing retrovirus partially restored intracellular TCRβ expression in DP and SP cells derived from LckCre-*Apc*$^{lox/lox468}$ and LckCre-*Ctnnb1*$^{+/lox(ex3)}$ mice. The fraction of cells that had undergone rearrangements and expressed TCRβ chains increased from 20.2% (uninfected) and 23.1% (EGFP alone) to 45.6% (NotchIC) for LckCre-*Ctnnb1*$^{+/lox(ex3)}$ thymocytes and from 21.8% (uninfected) to 49.8% (NotchIC) for LckCre-*Apc*$^{lox/lox468}$ thymocytes (Fig. 6). Similar infection of magnetically selected Cd25^{+} LckCre control thymocytes with retroviruses expressing NotchIC or EGFP alone did not substantially alter the fraction of DP and SP cells expressing intracellular TCRβ chains (Fig. 6). These findings indicate that β-catenin may ‘antagonize’ Notch signaling in immature thymocytes and that this crosstalk may affect *Tcrb* rearrangements.

Loss of APC prolongs the cell cycle and delays cytokinesis

The results presented above indicated that the loss of APC function ‘marked’ thymocyte development by several defects, which we also noted in mice with stabilized β-catenin.

However, only LckCre-*Apc*$^{lox/lox468}$ thymocytes seemed to have a blockade at the DN4 stage of development, which was reflected in a further reduced thymic cellularity. Those additional defects seemed to result from β-catenin-independent functions of APC. APC may be involved in chromosome segregation[10,11,39]. An inhibition in chromosome segregation could affect the length of the cell cycle and in this way result in a developmental block. To investigate whether immature thymocytes from LckCre-*Apc*$^{lox/lox468}$ mice cycled more slowly than their counterparts from LckCre or LckCre-*Ctnnb1*$^{+/lox(ex3)}$ mice, we sorted DN4 thymocytes from these mouse strains and stained them with carboxy-fluorescein diacetate succinamidyl ester (CFSE) before culturing the cells for 3 d with OP9-DL1 stromal cells[19]. After 3 d, we collected the nonadherent thymocytes and analyzed their proliferation index as well as progression to the DP and SP stages. Although the fraction of dividing cells in these cultures was similar for LckCre-*Apc*$^{lox/lox468}$ (89%), LckCre-*Ctnnb1*$^{+/lox(ex3)}$ (71%) and LckCre (76%) thymocytes, the average number of cell divisions after 3 d differed substantially for these cultures (Fig. 7). Whereas LckCre-*Ctnnb1*$^{+/lox(ex3)}$ and LckCre cells had undergone on average 3.32 and 3.34 cell divisions (proliferation index), respectively, LckCre-*Apc*$^{lox/lox468}$ cells had undergone an average of only 1.62 cell divisions ($P < 0.02$). This result indicates that one of the consequences of the loss of APC at the DN4 stage of thymocyte development is an increase in the overall length of the cell cycle. Developmental progression was also affected by the loss of APC. Whereas more than 90% of the LckCre control and LckCre-*Ctnnb1*$^{+/lox(ex3)}$ DN4 cells used to seed these cultures progressed to the DP and SP stages, more than 90% of the equivalent LckCre-*Apc*$^{lox/lox468}$ cells remained at the DN stages.

To determine which stage of the cell cycle was prolonged in LckCre-*Apc*$^{lox/lox468}$ thymocytes, we used cell cycle analyses. We sorted DN3 and DN4 thymocytes from LckCre-*Apc*$^{lox/lox468}$ and LckCre-*Ctnnb1*$^{+/lox(ex3)}$ mice and cultured them on OP9-DL1 cells, then blocked them in metaphase by treating them with colcemid. After ‘release’ from colcemid, DN thymocytes proceeded to cycle synchronously; however, LckCre-*Apc*$^{lox/lox468}$ cells exited mitosis approximately 12 h later than the equivalent LckCre-*Ctnnb1*$^{+/lox(ex3)}$ cells, indicating that the lengthening of the cell cycle in LckCre-*Apc*$^{lox/lox468}$ cells reflected a delay in the exit from mitosis (Fig. 8a). This finding was in line with evidence suggesting that APC may be involved in the regulation of mitotic checkpoints[10,11] and prompted us to specifically address mitotic defects in APC-deficient thymocytes. We therefore magnetically enriched samples from LckCre, LckCre-*Apc*$^{lox/lox468}$ and LckCre-*Ctnnb1*$^{+/lox(ex3)}$ mice for DN thymocytes and examined chromosome spreads banded with Giemsa-trypsin-Giemsa (GTG) as well as nuclei stained with 4′,6-diamidino-2-phenylindole. We used these preparations to visualize mitotic defects and abnormal chromosome content as well as accumulation of intrachromosomal translocations. Chromosome preparations from LckCre-*Apc*$^{lox/lox468}$ thymocytes but not from LckCre, or from LckCre-*Ctnnb1*$^{+/lox(ex3)}$ thymocytes had a distinct mitotic profile, with 20% of the dividing cells containing 80 condensed chromatids (Fig. 8b). This profile represents the stage immediately after sister chromatid separation and before cytokinesis. Normally cytokinesis proceeds rapidly after chromatid separation, rendering this stage undetectable in similar preparations of wild-type thymocytes. Detection of 80 chromatids indicated that loss of APC function in immature thymocytes introduced a delay in chromosome segregation. In addition to this defect in the

metaphase-to-anaphase transition, a greater proportion of DN LckCre-*Apc*$^{lox/lox468}$ thymocytes seemed to be aneuploid, probably because of aberrant sister chromatid segregation (Fig. 8c). However, GTG banding of chromosomes seemed normal for both LckCre-*Apc*$^{lox/lox468}$ and LckCre-*Ctnnb1*$^{+/lox(ex3)}$ DN thymocytes, indicating no substantial increase in intrachromosomal defects. Examination of nuclei stained with 4′,6-diamidino-2-phenylindole showed additional defects, such as anaphase bridges, which can result from unresolved chromatin Holliday recombination structures, as well as multipolar mitoses, albeit at lower frequencies (5 and 2 defects in 103 LckCre-*Apc*$^{lox/lox468}$ mitoses, respectively, compared with no abnormalities in 124 mitoses in LckCre controls; Supplementary Fig. 1 online). These observations indicated that loss of APC in DN thymocytes resulted in lengthening of the cell cycle, most likely because of a blockade of the metaphase-to-anaphase transition and chromosome segregation. These outcomes were independent of the stabilization of β-catenin.

DISCUSSION

Loss of APC function affects thymocyte development through two independent and conflicting molecular pathways, one involving the canonical Wnt–β-catenin signaling cascade and the other affecting chromosome segregation. Stabilization of β-catenin supports pre-TCR-independent thymocyte proliferation and promotes developmental progression without pre-TCR and αβ-TCR signaling. Here we have demonstrated that this aberrant differentiation involves inhibition of Notch-dependent transcription and suppression of *Tcrb* rearrangements in mice with active recombination-activating gene 1 and 2 proteins. Stabilization of β-catenin was a direct consequence of the loss of APC. Both the stabilization and ensuing molecular events were comparable in APC-deficient LckCre-*Apc*$^{lox/lox468}$ and β-catenin-stabilized LckCre-*Ctnnb1*$^{+/lox(ex3)}$ thymocytes, yet the absence of APC resulted in a substantial blockade in T cell development at the DN4 stage and extensive thymic atrophy. The blockade occurred at the level of chromosome segregation and resulted in prolongation of the cell cycle length. These *in vivo* observations demonstrate the disparity in the consequences of the loss of APC and stabilization of β-catenin in a developmental process that requires extensive cellular proliferation. Thymocytes that escaped the APC deficiency blockade were enriched for chromosomal abnormalities, emphasizing the vital function of APC in chromosome segregation and stability.

DN3 and DN4 thymocytes of both LckCre-*Apc*$^{lox/lox468}$ and LckCre-*Ctnnb1*$^{+/lox(ex3)}$ mice had reduced *Tcrb* V-to-DJ rearrangements. Recombination-activating gene–dependent *Tcr* rearrangement at the DN3 stage is the single most important event for further T cell maturation. In the mouse, *Tcrb* rearrangements are controlled by the *Tcrb* enhancer, located downstream of the constant 2 region of *Tcrb*[40]. As this fragment contains no consensus binding sites for Tcf-1 and Lef-1, the suppression of *Tcrb* VDJ-β rearrangements in LckCre-*Apc*$^{lox/lox468}$ and LckCre-*Ctnnb1*$^{+/lox(ex3)}$ thymocytes is unlikely to be a direct consequence of β-catenin signaling. We have provided evidence that this suppression may be due in part to the downregulation of Notch activity by β-catenin signaling.

In our studies, loss of APC function and stabilization of β-catenin correlated with suppression of several Notch-dependent transcripts at the DN4 stage of thymocyte

development, including *Notch1* and *Notch3* as well as the Notch targets *Hes1* and *Dtx1*. Conditional thymocyte-specific deletion of *Notch1* using the LckCre transgene has been reported to result in reduced VDJ-β rearrangements[21]. To link suppression of rearrangements with the modulation of Notch activity by β-catenin, we introduced NotchIC into immature LckCre-*Apc*$^{lox/lox468}$ and LckCre-*Ctnnb1*$^{+/lox(ex3)}$ thymocytes starting at the DN2 and DN3 stages and allowed them to differentiate in OP9-DL1 cocultures *in vitro*. Indeed, a substantial fraction of DP and SP cells developing from these retrovirus-transduced thymocytes had undergone *Tcrb* V-to-DJ rearrangements and expressed intracellular TCRβ chains. We conclude that crosstalk between β-catenin and Notch may affect at least in part *Tcrb* VDJ rearrangements.

Negative and positive genetic interactions between Notch and the analog of Wnt in *Drosophila melanogaster* (Wingless) are thought to be critical in many cell fate decisions[37]. Evidence in mouse systems has lent support to those proposals and has indicated involvement of Notch and Wnt interactions in the regulation of differentiation and self-renewal[34–36]. Our findings are in line with those proposals indicating antagonistic interaction between the Wnt–β-catenin and Notch activities in developing thymocytes.

As for the length of the cell cycle, DN4 thymocytes that lacked APC function underwent on average one to one-and-a-half fewer cell cycles than their LckCre or LckCre-*Ctnnb1*$^{+/lox(ex3)}$ counterparts in 3 d of culture together with OP9-DL1 cells. Cell cycle analyses indicated that this was due to a delayed exit from mitosis. One explanation for this is likely to be a delay in chromosome segregation. Evidence for such a delay was provided by the frequent detection of mitotic cells with 80 chromatids in DN thymocytes from LckCre-*Apc*$^{lox/lox468}$ mice. These cells represent the stage after chromatid separation and before cytokinesis. The rapid segregation of sister chromatids after separation to the opposite poles of the mitotic spindle renders this stage undetectable in normal thymocytes. The detection of this stage in LckCre-*Apc*$^{lox/lox468}$ DN thymocytes indicated defects in the meta-phase-to-anaphase transition resulting in inhibition of chromosome segregation. Involvement of APC in the control of chromosome segregation has been suggested by studies documenting localization of APC at the kinetochore during mitosis[10,11]. The exact function of APC at the kinetochore is not clearly understood. However, APC interacts with the microtubule end-binding protein EB1 (ref. 41). APC also binds to and stabilizes microtubules[42], localizes to the ends of microtubules embedded in kinetochores, forms a complex with mitotic checkpoint proteins Bub1 and Bub3 and is a substrate for both Bub1 and BubR1 kinases *in vitro*[10]. To ensure accurate segregation, the mitotic checkpoint acts to block entry into anaphase until both kinetochores of every duplicated chromatid pair have attached correctly to spindle microtubules. Accumulating evidence indicates that unattached kinetochores and/or those not under microtubule-induced tension mediate a ‘wait anaphase’ signal[43]. Anaphase ensues soon after the last kinetochore attaches to the spindle[44] and repeated detachment of a meiotic chromosome from a spindle by manipulation with a ‘micro-needle’ delays anaphase indefinitely[45]. APC might provide a non-motor-related functional link between the chromatids, microtubules and the components of the mitotic checkpoint. In that case, the absence of APC could result in a ‘wait anaphase’ signal similar to that of an unattached kinetochore.

Pre-TCR signaling is thought to promote the survival, proliferation and differentiation of immature thymocytes[46,47]. Moreover, the process of β-selection requires both Notch and pre-TCR signaling[48]. It is possible that concomitant inhibition of pre-TCR expression and Notch activity may have contributed to the reduced proliferation as well as increased apoptosis of LckCre-*Apc*$^{lox/lox468}$ and LckCre-*Ctnnb1*$^{+/lox(ex3)}$ DN4 thymocytes. Activated Wnt–β-catenin signaling in these abnormally developing thymocytes may bypass the differentiation signals attributed to the pre-TCR and Notch pathways but may only partially substitute for the proliferation and survival signals[26,48].

Our findings have indicated that loss of APC function poses a dilemma for the developing thymocyte. It stabilizes β-catenin, down-regulates Notch-dependent signaling, suppresses *Tcrb* rearrangements and allows for pre-TCR-independent proliferation and aberrant developmental progression. However, it also impairs the cell cycle by imposing a blockade in the metaphase-to-anaphase transition. A solution to this dilemma may be genetic instability and selection for mutations that alleviate the cell cycle block. Thus, whereas independent stabilization of β-catenin would be expected to lead to the accumulation of abnormal cells, it is the loss of APC that is likely to ‘select for’ malignancy.

METHODS

Mice

The generation and PCR genotyping of *Ctnnb1*$^{+/lox(ex3)}$ and LckCre mice has been described[30,31]. PCR genotyping of *Apc*$^{lox/lox468}$ mice and analysis of Cre-mediated deletion was done with the following primers: upstream primer p1 (5′-GTATTCTCAGTCTTAGCGTTCT-3′) was used in combination with downstream primer p2 (5′-TTAACAAGGGCAAAAGGAAACA-3′) to identify *lox*P-flanked and wild-type alleles and downstream prime p3 (5′-AATAAAAATAGGAATGCTCTGC-3′) to assess Cre-mediated deletion. All mice were maintained in specific pathogen–free animal facilities at the Tufts–New England Medical Center (Boston, Massachusetts) and were handled according to protocol 49-03 approved by the Institutional Animal Care and Use Committee of Tufts–New England Medical Center.

Flow cytometry and antibodies

Four-color flow cytometry staining was done as described[49]. The following monoclonal antibodies were purchased from BD PharMingen: anti-CD3 conjugated to phycoerythrin or biotin (17A2 and 500A2); anti-B220 conjugated to CyChrome (RA3.6B2); anti-CD4 conjugated to fluorescein isothiocyanate, CyChrome, phycoerythrin or allophycocyanin (RM4-5); anti-CD8 conjugated to fluorescein isothiocyanate, CyChrome, phycoerythrin or allophycocyanin (53.6.7); anti-TCRβ conjugated to phycoerythrin or CyChrome (H57); anti-TCR conjugated to fluorescein isothiocyanate or phycoerythrin or biotinylated (GL3); anti–pan NK conjugated to phycoerythrin or biotinylated (DX5); anti-CD44 conjugated to fluorescein isothiocyanate or phycoerythrin (IM7); anti-CD25 conjugated to allophycocyanin (PC61); anti-Gr1 conjugated to phycoerythrin or biotinylated (RB6.782); anti-CD11b conjugated to phycoerythrin or biotinylated (M1/70); and anti-Ter119 conjugated to phycoerythrin or biotinylated. Anti-β-catenin was purchased from BD

Transduction Laboratories. Biotinylated antibodies were visualized with streptavidin-phycoerythrin (Caltag), streptavidin-CyChrome (PharMingen) or streptavidin-allophycocyanin (Molecular Probes). The fluorescein isothiocyanate–annexin V labeling kit was from PharMingen. Cellular Bcl-2 expression was analyzed as recommended by the manufacturer using anti–murine Bcl-2 (monoclonal antibody 3F11; PharMingen) and purified hamster IgG (anti-trinitrophenol; PharMingen) as a negative control. For analysis of DN CD3 thymocytes, all cells expressing mature T cell or non–T cell markers were 'gated out' of the analyses using a pool of phycoerythrin-conjugated or biotinylated antibodies to CD4, CD8, TCRβ, TCRγδ, CD19, Gr1, Mac1, Ter119 and DX5 ('cocktail' of lineage-specific antibodies) that were visualized with streptavidin-CyChrome. Dead cells and debris were removed by appropriate gating of forward scatter and site scatter. Intracellular staining for TCRβ and β-catenin was done as described[26]. After surface staining, thymocyte subsets were fixed in 2% paraformaldehyde, then were stained with anti-TCRβ–phycoerythrin or anti-β-catenin in 0.1% saponin and 2% FCS in PBS. A Cyan flow cytometer (Dakocytomation) was used for flow cytometry and data were analyzed with FlowJo software (Tree Star).

For enrichment of samples for DN thymocyte subsets before cell sorting, cell suspensions were stained with the biotinylated 'cocktail' of lineage-specific antibodies, followed by incubation with streptavidin-conjugated magnetic beads (Dynal) and magnetic depletion of mature lineages. Enriched cell suspensions were then surface-stained with anti-CD44, anti-CD25 and streptavidin-CyChrome. Cell sorting was done with a MoFlo cell sorter (Dakocytomation).

Quantification of *Tcrb* rearrangements

DN3 and DN4 thymocytes (isolated and stained as described above) were sorted on a MoFlo cell sorter (DakoCytomation). PCR for *Tcrb* rearrangements and Thy-1 was done as described[33] on total cell lysates with the following primers: $D_\beta2$ (5′), 5′-GTAGGCACCTGTGGGGAAGAAACT-3′; $J_\beta2$ (3′), 5′-TGAGAGCTGTCTCC TACTATCGATT-3′; $V_\beta5.1$, 5′-GTCCAACAGTTTGATGACTATCAC-3′; $V_\beta8.2$, 5′-CCTCATTCTGGAGTTGGCTACCC-3′; 5′-*Thy1*, 5′-CCATCCAGCATGAGTTCAGC-3′; and 3′-*Thy1*, 5′-GCATCCAGGATGTGTTCTGA-3′. An OpticonII (MJ Research) was used for quantitative RT-PCR. Cell lysates were initially amplified in duplicate with the 5′-*Thy1* and 3′-*Thy1* primers to allow equilibration of the cell lysates with respect to DNA content. SYBR Green (Applied Biosystems) chemistry was used for reactions. The 1× reaction mixtures consisted of 7.5 μl 2× SYBR Green mix, 0.5 μl of each primer (10 pmol), distilled H_2O and cell lysate for a final volume of 15 μl. Equilibrated samples were then amplified in independent duplicate reactions with each of the $D_\beta2$-$J_\beta2$, $V_\beta5.1$-$J_\beta2$ and Vβ8.2-Jβ2 combination of primers. Amplification reactions with the 5′-*Thy1* and 3′-*Thy1* primers were included in each experiment as controls. The cycling conditions were 1 min at 94 °C, 2 min at 56 °C and 3 min at 68 °C. The course of the reactions was monitored in real time, and as soon amplification of the wild-type samples entered the linear phase, all reactions were stopped and products were separated by 1.2% agarose gel electrophoresis to visualize differences between the samples. In other experiments, reactions were allowed to reach completion (35 cycles), and a comparative threshold cycle value was chosen to fall within

the linear phase for each set of curves. The relative amplification for each of the experimental reactions was determined with the experimental comparative threshold values and amplification of the wild-type samples was considered to represent 100%.

Semiquantitative PCR

Cells were sorted and mRNA was extracted from up to 5×10^4 cells with the High Pure total mRNA isolation kit (Roche). The cDNA was prepared with Superscript II RT kit (Invitrogen). The amount of cDNA was quantified by amplification of *Actb* (encoding β-actin) using SYBR Green quantitative PCR and an OpticonII (MJ Research). The cDNA abundance was equilibrated and serial 1:5 dilutions were prepared. All PCR amplifications used 'touchdown' conditions with a reaction volume of 30 μl. Oligonucleotide primer sequences were as follows: *Notch1* forward, 5′-CGGTGTGAGGG TGATGTCAATG-3′, and *Notch1* reverse, 5′-GAATGTCCGGGCCAGC GCC ACC-3′; *Notch3* forward, 5′-GAGGCTACCTTGGCTCTGCT-3′, and *Notch3* reverse, 5′-GGCAGCCTGTCCAAGTGATCT-3′; *Dtx1* forward, 5′-CCCTCGCCACTGCTACCTA-3′, and *Dtx1* reverse, 5′-AAAGGGAAG GCGGGCAACTC-3′; *Hes1* forward, 5′-CAGCCAGTGTC AACACGACAC-3′, and *Hes1* reverse, 5′-TCGTTCATGCACTCGCTGAG-3′; *Actb* forward, 5′-TGG AATCCTGTGGCATCCATGAAAC-3′, and *Actb* reverse, 5′-TAAAACGCAGC TCAGTAA CAGTCCG-3′.

Chromosome spread preparations and GTG banding

For enrichment for DN thymocytes, thymocyte suspensions were incubated with the following biotin-conjugated antibodies: anti-CD4, anti-CD8, anti-TCRγδ, anti-NK1.1, anti-MacI and anti-Ter119. This was followed by incubation with streptavidin-conjugated magnetic beads (Dynal). The DN thymocytes obtained were then processed according to the standard methods and chromosome spreads were prepared and GTG-banded.

Retroviral transduction, CFSE labeling and OP9-DL1 stromal cultures

Thymocyte suspensions were prepared from four to five mice and were incubated for 20 min with biotinylated anti-CD25. Cell suspensions were washed to remove excess antibody and were incubated with streptavidin-conjugated MACS beads (Miltenyi Biotech). $CD25^+$ cells were selected from magnetic columns following the protocol recommended by the manufacturer. The selected cells (1×10^6 to 2×10^6 cells) were resuspended in 1 ml of αMEM supplemented with 20% FBS, penicillin-streptomycin, interleukin 7 (1 ng/ml), Flt3 ligand (5 ng/ml) and stem cell factor (5 ng/ml) and were preincubated for 3 h at 37 °C. A concentrated retroviral suspension (1×10^7 to 3×10^7 infectious units) and 6.7 μg/ml of polybrene were added to these preincubated cells, followed by 'spin infection' for 90 min at 2,500*g*. After 16–20 h, cells were stained with anti-CD25–allophycocyanin, anti-CD44–phycoerythrin and anti-CD4–CyChrome plus anti-CD8–CyChrome. $EGFP^+$ and $EGFP^-$ DN2 and DN3 cells were sorted independently and were cultured for 8–9 d with OP9-DL1 cells as described[19].

Sorted DN4 thymocytes were labeled with CFSE using a modification of a published method[50]. Sorted cells (1×10^6 to 1.5×10^6) were resuspended in 200 μl PBS supplemented

with 0.1% BSA and 5 μM CFSE. Cells were incubated in this solution for 10 min at 37 °C and then were washed extensively to eliminate the remaining CFSE. Viability after labeling exceeded 60%. CFSE-labeled cells were plated onto 10-cm tissue culture plates containing a confluent monolayer of OP9-GFP cells. Cocultures were done in the presence of 5 ng/ml of Flt3 ligand (Peprotech). Cocultures were collected 3 d later by 'shake-off' and careful pipetting to avoid inclusion of $EGFP^+$ GFP^+ OP9-DL1 stroma cells.

Single-cell suspensions obtained from age- and sex-matched mice were stained with anti-CD25–fluorescein isothiocyanate and anti-CD44–Cychrome as well as antibodies to lineage markers (CD4, CD8, CD44, B220, Mac-1, Ter119, Gr-1, DX5 and TCRγδ; all coupled to phycoerythrin). DN3 and DN4 populations were sorted with a MoFlo (Dakocytomation), were pooled and were labeled with anti-CD45–phycoerythrin. Of these pools, 3×10^5 cells were plated in each well of a six-well dish containing a monolayer of OP9-DL1 stroma cells[19]. For synchronization, cells were kept overnight in α-MEM (Gibco Invitrogen) containing 20% FBS and 1 μg/ml of colcemid (Sigma Aldrich). The following morning, cultures were 'released' from colcemid into α-MEM containing 20% FBS and 5 ng/ml of Flt3 ligand. Cell cycle analyses were made every 4 h. Cells from individual wells were collected by vigorous pipetting and were stained for 1 h at 4 °C in the dark with 20 μl 7AAD (Becton Dickinson) in 100 μl PBS containing 2% FBS and 0.04% saponin. Samples were washed and were analyzed by flow cytometry. Gated $CD45^+$ cells were analyzed for the percentages of cells in the S-G2-M phases.

Supplementary Material

Refer to Web version on PubMed Central for supplementary material.

Acknowledgments

The authors thank J.C. Zúñiga-Pflücker (University of Toronto, Toronto, Canada) for advice, support and the OP9-DL1 cells; I. Khan for help with the OP9-DL1 cultures; K. Georgopoulos (Massachusetts General Hospital), P. Sicinski and R. Van Etten for critical comments on the manuscript; I. Aifantis (University of Chicago), X. Li and A. Campese for the NotchIC retrovirus; and H. von Boehmer and R.M. Meyer for their interest and support. Supported by the National Institutes of Health (R01 AI059676-01 to F.G. and R01 CA104547-01A1 to K.K.), the Medical Foundation (Smith Family New Investigator Award to F.G.), the Dana Farber Cancer Institute (National Colorectal Cancer Research Alliance Award to K.K.) and the Claudia Adams Barr Program (K.K.).

References

1. van de Wetering M, de Lau W, Clevers H. WNT signaling and lymphocyte development. Cell. 2002; 109:S13–S19. [PubMed: 11983149]
2. Morin PJ, et al. Activation of β-catenin-Tcf signaling in colon cancer by mutations in β-catenin or Apc. Science. 1997; 275:1787–1790. [PubMed: 9065402]
3. Smits R, et al. Apc1638N: a mouse model for familial adenomatous polyposis-associated desmoid tumors and cutaneous cysts. Gastroenterology. 1998; 114:275–283. [PubMed: 9453487]
4. Sparks AB, Morin PJ, Vogelstein B, Kinzler KW. Mutational analysis of the APC/β-catenin/Tcf pathway in colorectal cancer. Cancer Res. 1998; 58:1130–1134. [PubMed: 9515795]
5. Miyoshi Y, et al. Germ-line mutations of the *Apc* gene in 53 familial adenomatous polyposis patients. Proc Natl Acad Sci USA. 1992; 89:4452–4456. [PubMed: 1316610]
6. Powell SM, et al. Molecular diagnosis of familial adenomatous polyposis. N Engl J Med. 1993; 329:1982–1987. [PubMed: 8247073]

7. Miyaki M, et al. Coexistence of somatic and germ-line mutations of APC gene in desmoid tumors from patients with familial adenomatous polyposis. Cancer Res. 1993; 53:5079–5082. [PubMed: 8221638]
8. Korinek V, et al. Constitutive transcriptional activation by a β-catenin-Tcf complex in $APC^{-/-}$ colon carcinoma. Science. 1997; 275:1784–1787. [PubMed: 9065401]
9. Shih IM, et al. Top-down morphogenesis of colorectal tumors. Proc Natl Acad Sci USA. 2001; 98:2640–2645. [PubMed: 11226292]
10. Kaplan KB, et al. A role for the Adenomatous Polyposis Coli protein in chromosome segregation. Nat Cell Biol. 2001; 3:429–432. [PubMed: 11283619]
11. Fodde R, et al. Mutations in the APC tumour suppressor gene cause chromosomal instability. Nat Cell Biol. 2001; 3:433–438. [PubMed: 11283620]
12. Martin CH, et al. Efficient thymic immigration of $B220^{+}$ lymphoid-restricted bone marrow cells with T precursor potential. Nat Immunol. 2003; 4:866–873. [PubMed: 12925850]
13. Shortman K, Wu L. Early T lymphocyte progenitors. Annu Rev Immunol. 1996; 14:29–47. [PubMed: 8717506]
14. Allman D, et al. Thymopoiesis independent of common lymphoid progenitors. Nat Immunol. 2003; 4:168–174. [PubMed: 12514733]
15. Schwarz BA, Bhandoola A. Circulating hematopoietic progenitors with T lineage potential. Nat Immunol. 2004; 5:953–960. [PubMed: 15300246]
16. Kondo M, Weissman IL, Akashi K. Identification of clonogenic common lymphoid progenitors in mouse bone marrow. Cell. 1997; 91:661–672. [PubMed: 9393859]
17. Porritt HE, et al. Heterogeneity among DN1 prothymocytes reveals multiple progenitors with different capacities to generate T cell and non-T cell lineages. Immunity. 2004; 20:735–745. [PubMed: 15189738]
18. Radtke F, et al. Deficient T cell fate specification in mice with an induced inactivation of Notch1. Immunity. 1999; 10:547–558. [PubMed: 10367900]
19. Schmitt TM, Zuniga-Pflucker JC. Induction of T cell development from hematopoietic progenitor cells by delta-like-1 *in vitro*. Immunity. 2002; 17:749–756. [PubMed: 12479821]
20. von Boehmer H. Aspects of lymphocyte developmental biology. Immunol Today. 1997; 18:260–262. [PubMed: 9190108]
21. Wolfer A, Wilson A, Nemir M, MacDonald HR, Radtke F. Inactivation of Notch1 impairs VDJβ rearrangement and allows pre-TCR-independent survival of early αβ Lineage Thymocytes. Immunity. 2002; 16:869–879. [PubMed: 12121668]
22. Schilham MW, et al. Critical involvement of Tcf-1 in expansion of thymocytes. J Immunol. 1998; 161:3984–3991. [PubMed: 9780167]
23. Ioannidis V, Beermann F, Clevers H, Held W. The β-catenin–TCF-1 pathway ensures $CD4^{+}CD8^{+}$ thymocyte survival. Nat Immunol. 2001; 2:691–697. [PubMed: 11477404]
24. Okamura RM, et al. Redundant regulation of T cell differentiation and TCRα gene expression by the transcription factors LEF-1 and TCF-1. Immunity. 1998; 8:11–20. [PubMed: 9462507]
25. Xu Y, Banerjee D, Huelsken J, Birchmeier W, Sen JM. Deletion of β-catenin impairs T cell development. Nat Immunol. 2003; 4:1177–1182. [PubMed: 14608382]
26. Gounari F, et al. Somatic activation of β-catenin bypasses pre-TCR signaling and TCR selection in thymocyte development. Nat Immunol. 2001; 2:863–869. [PubMed: 11526403]
27. Fodde R, et al. A targeted chain-termination mutation in the mouse *APC* gene results in multiple intestinal tumors. Proc Natl Acad Sci USA. 1994; 91:8969–8973. [PubMed: 8090754]
28. Moser AR, Pitot HC, Dove WF. A dominant mutation that predisposes to multiple intestinal neoplasia in the mouse. Science. 1990; 247:322–324. [PubMed: 2296722]
29. Oshima M, et al. Loss of Apc heterozygosity and abnormal tissue building in nascent intestinal polyps in mice carrying a truncated *Apc* gene. Proc Natl Acad Sci USA. 1995; 92:4482–4486. [PubMed: 7753829]
30. Harada N, et al. Intestinal polyposis in mice with a dominant stable mutation of the β-catenin gene. EMBO J. 1999; 18:5931–5942. [PubMed: 10545105]

31. Lee PP, et al. A critical role for Dnmt1 and DNA methylation in T cell development, function, and survival. Immunity. 2001; 15:763–774. [PubMed: 11728338]
32. Moore NC, Anderson G, Williams GT, Owen JJ, Jenkinson EJ. Developmental regulation of bcl-2 expression in the thymus. Immunology. 1994; 81:115–119. [PubMed: 8132207]
33. Anderson SJ, Abraham KM, Nakayama T, Singer A, Perlmutter RM. Inhibition of T-cell receptor β-chain gene rearrangement by overexpression of the non-receptor protein tyrosine kinase p56lck. EMBO J. 1992; 11:4877–4886. [PubMed: 1334460]
34. Duncan AW, et al. Integration of Notch and Wnt signaling in hematopoietic stem cell maintenance. Nat Immunol. 2005; 6:314–322. [PubMed: 15665828]
35. Galceran J, Sustmann C, Hsu SC, Folberth S, Grosschedl R. LEF1-mediated regulation of Delta-like1 links Wnt and Notch signaling in somitogenesis. Genes Dev. 2004; 18:2718–2723. [PubMed: 15545629]
36. Nicolas M, et al. Notch1 functions as a tumor suppressor in mouse skin. Nat Genet. 2003; 33:416–421. [PubMed: 12590261]
37. Martinez Arias A. Interactions between Wingless and Notch during the assignment of cell fates in *Drosophila*. Int J Dev Biol. 1998; 42:325–333. [PubMed: 9654016]
38. Sicinska E, et al. Requirement for cyclin D3 in lymphocyte development and T cell leukemias. Cancer Cell. 2003; 4:451–461. [PubMed: 14706337]
39. Aoki K, Tamai Y, Horiike S, Oshima M, Taketo MM. Colonic polyposis caused by mTOR-mediated chromosomal instability in $Apc^{+/\Delta 716}$ $Cdx2^{+/-}$ compound mutant mice. Nat Genet. 2003; 35:323–330. [PubMed: 14625550]
40. McDougall S, Peterson CL, Calame K. A transcriptional enhancer 3′ of C β 2 in the T cell receptor β locus. Science. 1988; 241:205–208. [PubMed: 2968651]
41. Su LK, et al. APC binds to the novel protein EB1. Cancer Res. 1995; 55:2972–2977. [PubMed: 7606712]
42. Zumbrunn J, Kinoshita K, Hyman AA, Nathke IS. Binding of the adenomatous polyposis coli protein to microtubules increases microtubule stability and is regulated by GSK3 β phosphorylation. Curr Biol. 2001; 11:44–49. [PubMed: 11166179]
43. Cleveland DW, Mao Y, Sullivan KF. Centromeres and kinetochores: from epigenetics to mitotic checkpoint signaling. Cell. 2003; 112:407–421. [PubMed: 12600307]
44. Rieder CL, Schultz A, Cole R, Sluder G. Anaphase onset in vertebrate somatic cells is controlled by a checkpoint that monitors sister kinetochore attachment to the spindle. J Cell Biol. 1994; 127:1301–1310. [PubMed: 7962091]
45. Li X, Nicklas RB. Mitotic forces control a cell-cycle checkpoint. Nature. 1995; 373:630–632. [PubMed: 7854422]
46. Fehling HJ, Krotkova A, Saint-Ruf C, von Boehmer H. Crucial role of the pre-T-cell receptor α gene in development of αβ but not γδ T cells. Nature. 1995; 375:795–798. [PubMed: 7596413]
47. Hoffman ES, et al. Productive T-cell receptor β-chain gene rearrangement: coincident regulation of cell cycle and clonality during development *in vivo*. Genes Dev. 1996; 10:948–962. [PubMed: 8608942]
48. Ciofani M, et al. Obligatory role for cooperative signaling by pre-TCR and Notch during thymocyte differentiation. J Immunol. 2004; 172:5230–5239. [PubMed: 15100261]
49. Gounari F, et al. Tracing lymphopoiesis with the aid of a pTα-controlled reporter gene. Nat Immunol. 2002; 3:489–496. [PubMed: 11927910]
50. Hodgkin PD, et al. The importance of efficacy and partial agonism in evaluating models of B lymphocyte activation. Int Rev Immunol. 1997; 15:101–127. [PubMed: 9178074]

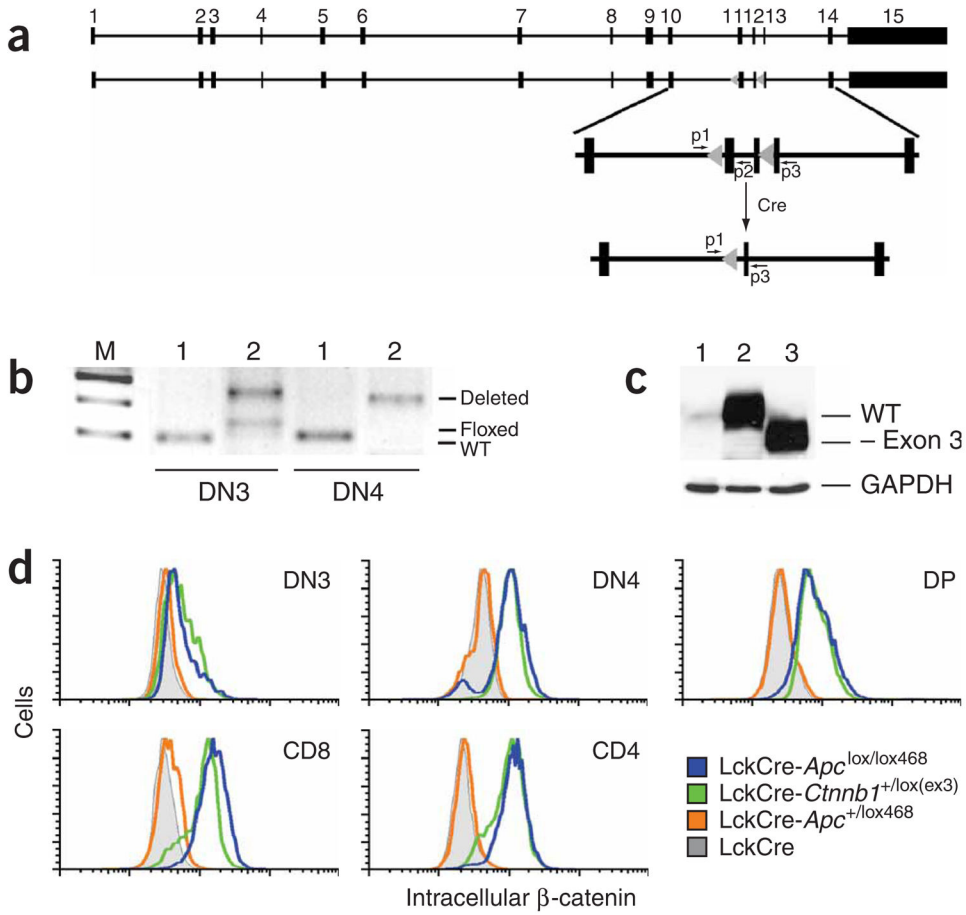

Figure 1.

Conditional *Apc* ablation in mouse thymocytes. (**a**) Wild-type *Apc* (above) and the *Apc*^{lox468} loci (below). Rectangles numbered 1–15 indicate the position of the exons. Below, enlargement of the region containing the lox*P* sites (gray arrowheads); bottom, the structure of the locus after Cre-mediated deletion. Small arrows labeled p1 and p2 indicate the position and the orientation of the primers used to detect the *lox*P-flanked allele; the small arrow labeled p3 indicates the position and the orientation of the primer used to detect Cre-mediated deletion.

(**b**) Course of LckCre-mediated deletion of *Apc*^{lox468} in developing thymocytes. DN3 and DN4 thymocytes from LckCre mice (lanes 1) and LckCre-*Apc*$^{lox/lox468}$ mice (lanes 2) were sorted independently and DNA was amplified by PCR using primers p1, p2 and p3. WT, wild-type allele; Floxed, *lox*P-flanked allele; Deleted, deletion of allele; M, molecular size marker. (**c**) Immunoblot analysis of total thymocyte lysates from LckCre (lane 1), LckCre-*Apc*$^{lox/lox468}$, (lane 2) and LckCre-*Ctnnb1*$^{+/lox(ex3)}$ (lane 3) mice using anti-β-catenin. WT, wild-type β-catenin; – Exon 3, protein encoded by gene lacking exon 3; GAPDH, loading control. Representative of three independent experiments. (**d**) Expression of β-catenin in various thymocyte subsets. Thymocytes were surface-stained with the ‘cocktail’ of lineage-specific antibodies (Methods) as well as with anti-CD44–phycoerythrin and anti-CD25–

allophycocyanin. Cells were then permeabilized and stained with anti-β-catenin–fluorescein isothiocyanate. Data are representative of five independent experiments.

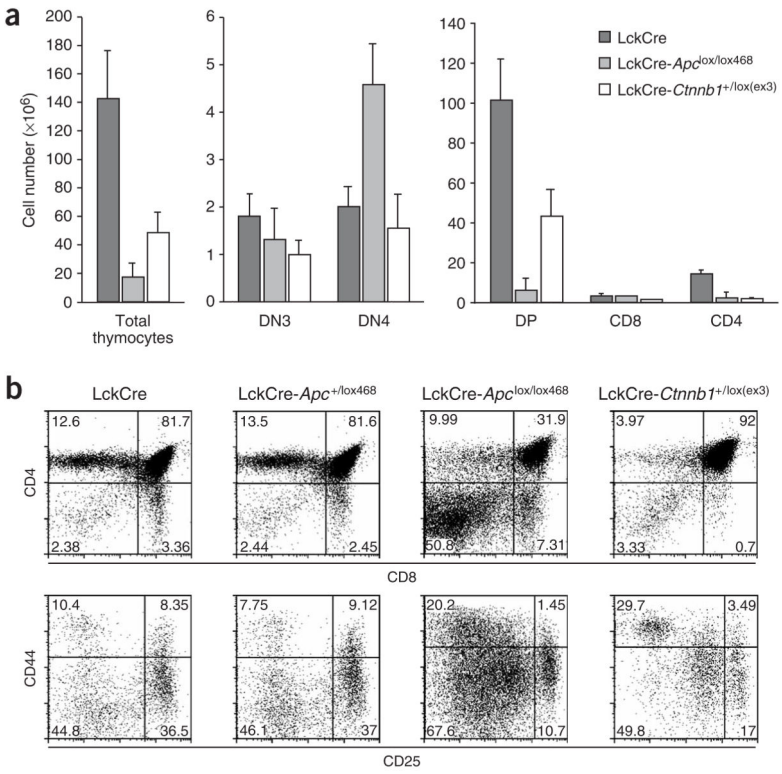

Figure 2.

Mice with conditional *Apc* deficiency have reduced thymic cellularity and a blockade at the DN4 stage of thymocyte development. (**a**) Thymic cellularity, estimated by calculation of the number of thymocytes from individual thymi after electronic gating of various subsets. Cell numbers were extrapolated from the percentage of each subset and the total number of thymocytes. Error bars represent the standard deviation of values obtained from different mice. Data represent the average values of nine LckCre-*Apc*$^{lox/lox468}$ and five LckCre mice as well as five age-matched LckCre-*Ctnnb1*$^{+/loxex3}$ mice. LckCre-*Apc*$^{lox/lox468}$ mice have significantly more DN4 thymocytes than do LckCre ($P < 0.07$) or LckCre-*Ctnnb1*$^{+/loxex3}$ ($P < 0.037$) mice.

(**b**) Thymocyte suspensions were stained with anti-CD4 and anti-CD8 (top row) or with a ‘cocktail’ of lineage-specific antibodies and anti-CD44 and anti-CD25 (bottom row). Lineage-positive cells were electronically ‘gated out’ and the CD44-versus-CD25 profiles of the lineage-negative subsets are presented (bottom row). Numbers in quadrants indicate the percentage of cells in each.

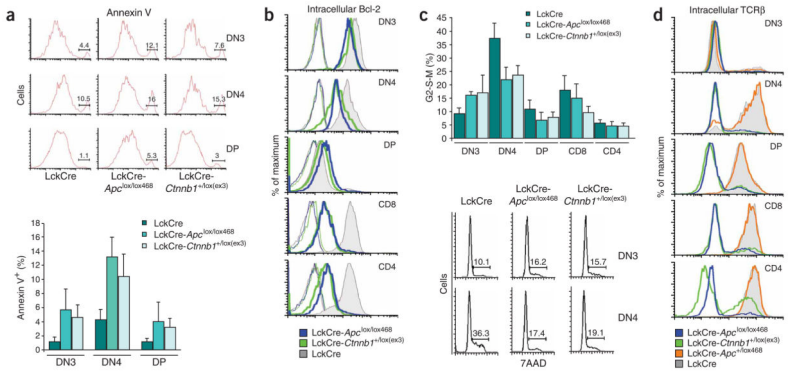

Figure 3.

Survival and proliferation of APC deficient thymocytes. (**a**) Apoptosis rates of immature thymocytes (DN3, DN4 and DP stages). Thymocyte suspensions were stained with cell surface markers and annexin V. Electronically gated cells were 'plotted' to detect annexin V–positive cells; numbers above bracketed lines indicate the percent of annexin V–positive cells. Bottom, cumulative data from five similar independent experiments. The increased apoptotic rates for LckCre-*Apc*$^{lox/lox468}$ and LckCre-*Ctnnb1*$^{+/lox(ex3)}$ thymocytes at the DN3 ($P < 0.012$ and $P < 0.07$, respectively), DN4 ($P < 0.0002$ and $P < 0.07$, respectively) and DP ($P < 0.075$ and $P < 0.023$, respectively) stages are statistically significant (Student's *t*-test). (**b**) Bcl-2 expression. Thymocytes were surface-stained with anti-CD4, anti-CD8 and anti-TCRβ or with the 'cocktail' of lineage-specific antibodies (Methods) combined with anti-CD44 and anti-CD25, followed by intracellular staining with anti-Bcl-2 (thick lines). Thin lines represent basal staining with an isotype control antibody. The CD4 and CD8 subsets of LckCre-*Apc*$^{lox/lox468}$ and LckCre-*Ctnnb1*$^{+/lox(ex3)}$ include only the abnormal TCRβ^{-} thymocytes, which represent most cells in these subsets of this mouse strains. (**c**) Proliferation rates of thymocyte subsets. Thymocyte suspensions were surface-stained before permeabilization and staining with 7AAD. Electronically gated thymocyte subsets were 'plotted' for 7AAD staining (bottom); bars represent the averaged values of five independent experiments; error bars represent standard deviation. For LckCre-*Apc*$^{lox/lox468}$ and LckCre-*Ctnnb1*$^{+/lox(ex3)}$ thymocytes, the increase in proliferation at the DN3 stage ($P < 0.0001$ and $P < 0.02$, respectively) and decrease in proliferation at the DN4 stage ($P < 0.0002$ and $P < 0.004$, respectively) is statistically significant. (**d**) Intracellular TCRβ expression. Thymocytes were surface-stained with anti-CD4 and anti-CD8 or with the 'cocktail' of lineage-specific antibodies (Methods) combined with anti-CD44 and anti-CD25 to identify the various thymocyte subsets, followed by intracellular staining with anti-TCRβ. Data are representative of more than five independent experiments.

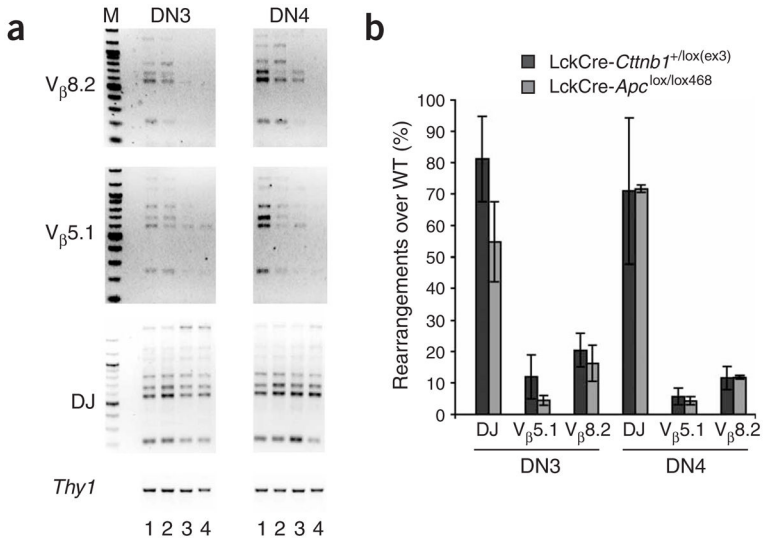

Figure 4.

Suppression of *Tcrb* VDJ rearrangements after ablation of APC or stabilization of β-catenin. (**a**) Limiting PCR of DNA from cell lysates of sorted DN3 or DN4 thymocytes derived from LckCre mice (lane 1), Lckcre-*Apc*$^{+/lox468}$ mice (lane 2), LckCre-*Ctnnb1*$^{+/lox(ex3)}$ mice (lane 3) and LckCre-*Apc*$^{lox/lox468}$ mice (lane 4). Data represent DJ and VDJ rearrangements. *Thy1*, quantity control (PCR of the same lysates). M, size marker.

(**b**) Quantification of the rearrangement in sorted DN3 and DN4 thymocytes based on SYBR Green incorporation in real-time PCR experiments. SYBR Green results for the wild-type (WT; LckCre) subsets are considered to be 100%. The calculated percentages represent the average of four independent experiments; error bars represent standard deviation values.

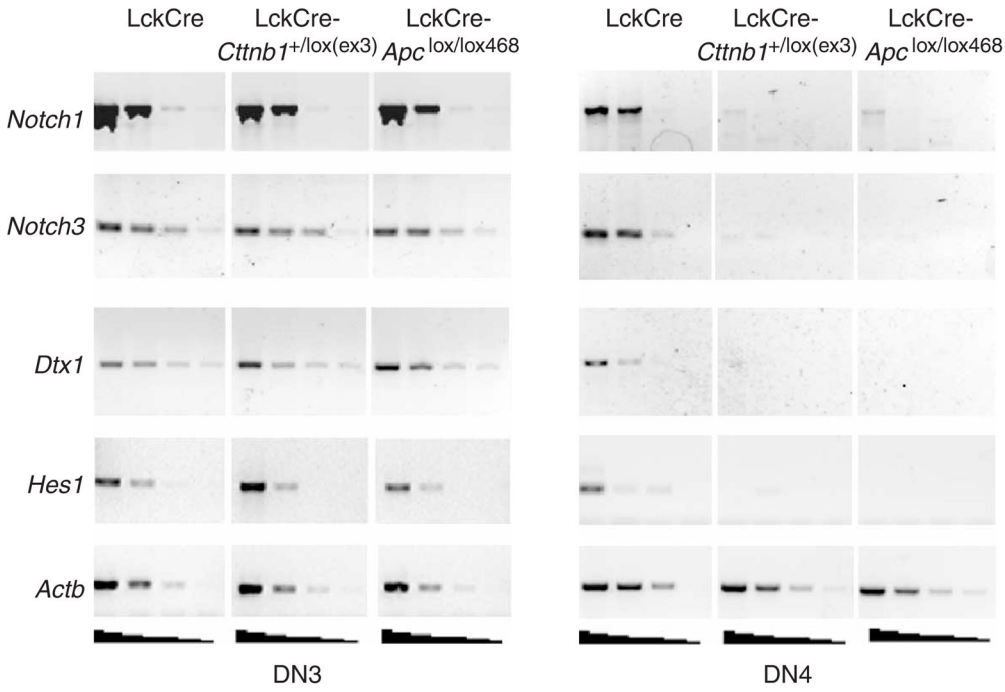

Figure 5.

Suppression of Notch activity by APC truncation and stabilization of β-catenin. Semiquantitative RT-PCR of serial dilutions of cDNA (fivefold increments per dilution; wedges) of cell lysates from sorted DN3 or DN4 thymocytes. Primers were specific for *Notch1*, *Notch3*, *Dtx1* and *Hes1*. *Actb*, quantity control. Results are representative of two independent preparations of sorted cells.

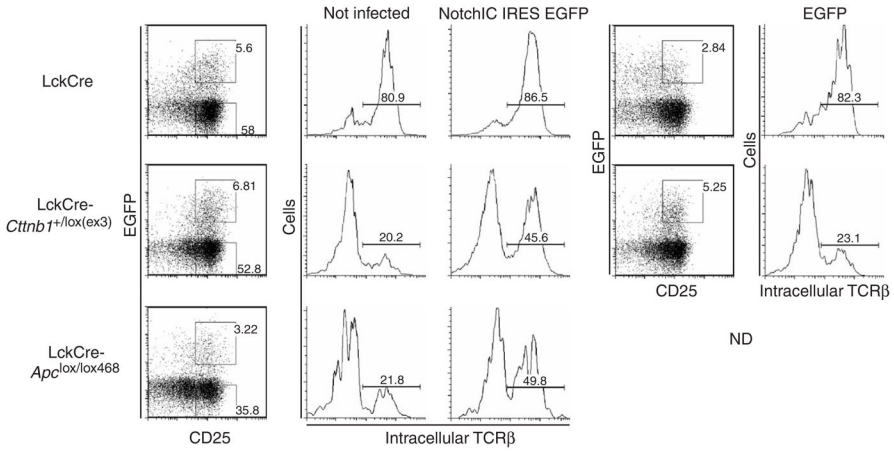

Figure 6.

Expression of activated Notch1 partially restores intracellular TCRβ expression in LckCre-*Apc*$^{lox/lox468}$ and LckCre-*Ctnnb1*$^{+/lox(ex3)}$ thymocytes differentiating on OP9-DL1 stroma cells. CD25^{+} thymocytes selected by magnetic beads were left uninfected or were infected with retroviruses expressing NotchIC in the context of a bicistronic construct with EGFP or only EGFP. Infected cells were stained with anti-CD4, anti-CD8 and anti-CD25. Dot plots show CD25-versus-EGFP staining of electronically gated DN cells subjected to sorting. Outlining indicates sorting gates; numbers beside outlined areas indicate the fraction of sorted cells. Sorted cells (5×10^4 to 1×10^5) from each population were plated on OP9-DL1 cells and were allowed to differentiate for 9 d, then were stained with anti-CD45, anti-CD4 and anti-CD8 followed by intracellular staining with anti-TCRβ and flow cytometry. Histograms show intracellular TCRβ expression of gated SP and DP cells derived from EGFP^{+} (Not infected), EGFP^{+} Notch-expressing cells (NotchIC IRES EGFP)and EGFP^{+} control retrovirus–infected cells (EGFP). Numbers above bracketed lines indicate the percent of cells with intracellular TCRβ^{+} chains. Data are representative of three independent experiments.

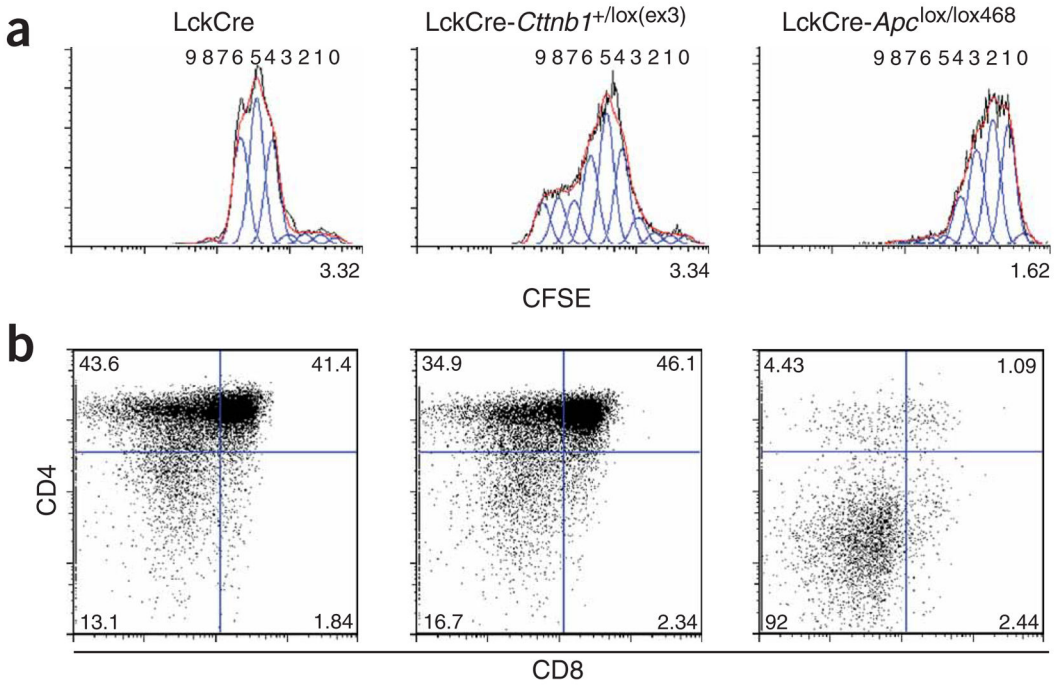

Figure 7.

LckCre-*Apc*$^{lox/lox468}$ DN4 thymocytes divide and differentiate more slowly than LckCre or LckCre-*Ctnnb1*$^{+/lox(ex3)}$ DN4 thymocytes on OP9-DL1 stroma cells. Sorted DN4 thymocytes were labeled with CFSE and plated onto OP9-DL1 stroma cells. After 3 d in culture, nonadherent cells were isolated, stained with anti-CD4 and anti-CD8 and analyzed for proliferation index (**a**) and developmental progression (**b**). (**a**) Numbers of cell divisions (at top) were calculated using FloJo software with the same constraints for all samples, including the same ratio between subsequent peaks as well as the same width for individual peaks. Proliferation indexes (below histograms) were calculated by FlowJo software on the basis of these set parameters. The reduction in the proliferation index of LckCre-*Apc*$^{lox/lox468}$ DN4 thymocytes is statistically significant ($P < 0.02$; paired analyses). (**b**) Numbers in quadrants indicate the percentage of cells in each. Data are representative of three experiments.

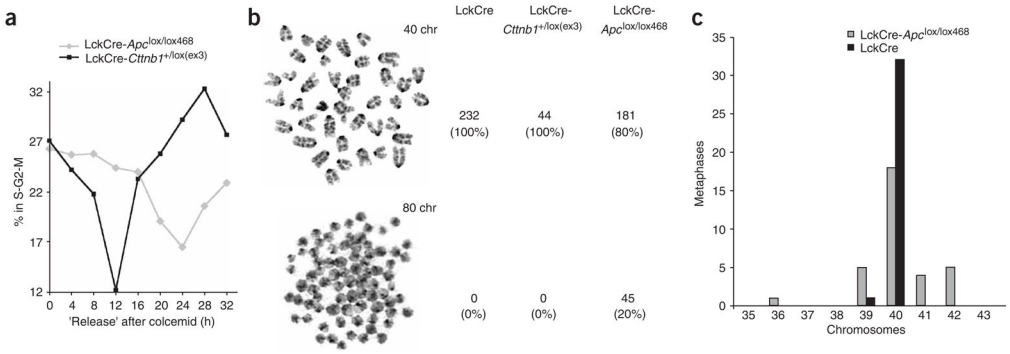

Figure 8.

Ablation of APC results in inhibition of chromosome segregation after chromatide separation and the accumulation of cells with aberrant chromosome numbers. (**a**) Cell cycle analysis of LckCre-*Apc*$^{lox/lox468}$ and LckCre-*Ctnnb1*$^{+/lox(ex3)}$ DN3 and DN4 thymocytes. Sorted thymocytes were cultured on OP9-DL1 cells overnight in the presence of colcemid and then were ‘released’ into normal culture medium, were permeabilized and were stained with 7AAD. The fraction of mitotic cells determined by flow cytometry is plotted against the time of incubation after ‘release’ from colcemid treatment.

(**b**) Chromosome spreads and GTG-banded magnetically depleted DN thymocytes. Top, metaphasic cell; bottom, distinct dividing profile seen only in LckCre-*Apc*$^{lox/lox468}$ thymocytes. chr, chromatid. Right, quantification of the number of dividing cells and the percentage of each mitotic phenotype. (**c**) Chromosomal content of DN thymocytes. LckCre-*Apc*$^{lox/lox468}$ dividing cells with the 80-chromatid phenotype were excluded from these calculations. Similar results were obtained for four independent chromosome preparations.